Cation Permeability and Cation-Anion Interactions in a Mutant GABA-Gated Chloride Channel from *Drosophila*

Chih-Tien Wang,* Hai-Guang Zhang,* Thomas A. Rocheleau,§ Richard H. ffrench-Constant,§ and Meyer B. Jackson*
Departments of *Physiology and §Entomology, University of Wisconsin–Madison, Madison, Wisconsin 53706 USA

ABSTRACT To investigate the structural basis of anion selectivity of *Drosophila* GABA-gated Cl^- channels, the permeation properties of wild-type and mutant channels were studied in *Xenopus* oocytes. This work focused on asparagine 319, which by homology is one amino acid away from a putative extracellular ring of charge that regulates cation permeation in nicotinic receptors. Mutation of this residue to aspartate reduced channel conductance, and mutation to lysine or arginine increased channel conductance. These results are consistent with an electrostatic interaction between this site and permeating anions. The lysine mutant, but not the arginine mutant, formed a channel that is permeable to cations, and this cannot be explained in terms of electrostatics. The lysine mutant had a 25-mV reversal potential in solutions with symmetrical Cl^- and asymmetrical cations. The permeability ratio of K^+ to Cl^- was determined as 0.33 from reversal potential measurements in KCl gradients. Experiments with large organic cations and anions showed that cation permeation can only be seen in the presence of Cl^-, but Cl^- permeation can be seen in the absence of permeant cations. Measurements of permeability ratios of organic anions indicated that the lysine mutant has an increased pore size. The cation permeability of the lysine-containing mutant channel cannot be accounted for by a simple electrostatic interaction with permeating ions. It is likely that lysine substitution causes a structural change that extends beyond this one residue to influence the positions of other channel-forming residues. Thus protein conformation plays an important role in enabling ion channels to distinguish between anions and cations.

INTRODUCTION

The nicotinic acetylcholine receptors and $GABA_A$ receptors are structurally homologous proteins that form channels with different ion selectivities. The homology between these proteins extends to the regions that form the ion conductive pore, raising the question of how cations and anions are distinguished and filtered. In the case of the nicotinic receptor, the cation conductance is especially sensitive to the presence of negative charge at three locations in and adjacent to M2 (Imoto et al., 1988; Lester, 1992) (Fig. 1). M2 is the second of four putative membrane-spanning segments of subunits in the ACh/GABA receptor channel family, and these segments are thought to surround the central aqueous channel (Lester, 1992; Karlin and Akabas, 1995). The acidic residues highlighted in Fig. 1 have been proposed to form negatively charged rings within the pore (Imoto et al., 1988).

Although these negatively charged rings in the nicotinic receptor interact with permeating cations, their role in charge selectivity has been difficult to establish. Mutations in the intermediate and outer rings of the nicotinic receptor α_7 subunit to neutral amino acids do not result in anion permeability (Galzi et al., 1992). The anion selective $GABA_A$ receptor does not have basic residues at the positions homologous to the intracellular and intermediate rings. (A pileup of 58 aligned sequences of vertebrate $GABA_A$ receptors prepared by Dr. Drew Boileau was examined.) In fact, the location corresponding to the intracellular ring has an acidic residue in many $GABA_A$ receptor subunits (e.g., rat α_1 in Fig. 1).

In the present study we focused on the role of a residue adjacent to the outer, extracellular ring at the C-terminal end of the M2 segment. The reason for selecting this residue is that in many $GABA_A$ receptor subunits this position is occupied by a basic amino acid (e.g., arginine in the $GABA_A$ α_1 subunit in Fig. 1). The strategic location of this residue near a ring of charge in the nicotinic receptor raises the possibility of an electrostatic interaction with permeating anions. Glycine receptors also contain an arginine at this position, and the channel conductance was reduced somewhat by replacing this arginine with glutamine or leucine (Langosch et al., 1994). However, another study suggested that mutations at this location altered agonist sensitivity rather than ion selectivity (Rajendra et al., 1994). We examined the role of this residue, using site-directed mutagenesis in a *Drosophila* GABA receptor encoded by the *Rdl* gene (resistance to dieldrin) (ffrench-Constant et al., 1991). This protein forms a GABA-gated Cl^- channel and is structurally related to vertebrate $GABA_A$ and glycine receptors. When mutated at position 302 from alanine to serine (Fig. 1), the receptor becomes resistant to cyclodiene insecticides (e.g., dieldrin) and the convulsant drug picrotoxin (ffrench-Constant et al., 1993; Zhang et al., 1994). High channel activity is achieved in heterologous systems expressing just the *Rdl* gene product, indicating that this

Received for publication 23 July 1998 and in final form 16 April 1999.

Address reprint requests to Dr. Meyer Jackson, Department of Physiology, SMI 127, University of Wisconsin Medical School–Madison, 1300 University Ave., Madison, WI 53706. Tel.: 608-262-9111; Fax: 608-265-5512; E-mail: mjackson@physiology.wisc.edu.

Dr. Zhang's present address is Department of Genetics, University of California, Berkeley, CA 74720.

0006-3495/99/08/691/10 $2.00

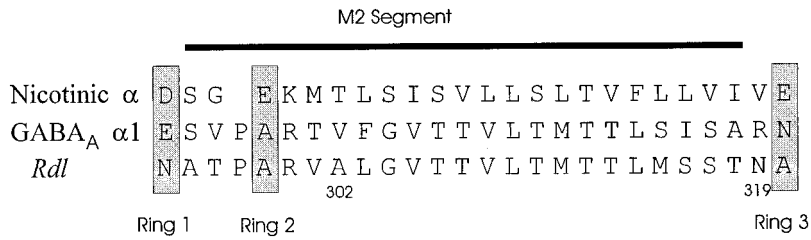

FIGURE 1 Aligned sequences are shown for M2 segments and flanking residues of 1) the *Torpedo* nicotinic receptor α subunit, 2) the rat $GABA_A$ receptor α_1 subunit, and 3) the *Rdl* gene product. The M2 segment is indicated by the bar above. Rings of charge influencing the cation permeability of the nicotinic receptor (Imoto et al., 1988) are shaded, along with the homologous residues of the two GABA receptors shown. Note that N319 of the *Rdl* gene product was the site mutated in the present study. In cyclodiene-sensitive receptors residue 302 is alanine; in cyclodiene-resistant receptors residue 302 is serine.

subunit has the capacity to assemble as a homomultimer (ffrench-Constant et al., 1993; Lee et al., 1993; Zhang et al., 1995). This channel thus has the advantage that mutations introduced by site-directed mutagenesis will appear in all of the subunits. The *Rdl* protein contains an asparagine (N319) at the location of interest (Fig. 1). We found in some instances that charge at this location influenced anion conductance in the expected manner. However, mutations at this site had a number of additional unexpected consequences that are not easily explained in terms of electrostatics. These results indicate that N319 contributes to the maintenance of a conformation that ensures anion selectivity. These conformational effects determine whether the channel completely excludes cations or allows the passage of cations by a complex mechanism that may involve interactions with anions.

MATERIALS AND METHODS

Site-directed mutagenesis

The cloning of the *Drosophila Rdl* GABA receptor has been described previously (ffrench-Constant et al., 1991). In the present study, we used both wild-type *Rdl* cDNA pNB14.1 (referred to here as Rdl^S) and cDNA carrying the A302S mutation responsible for cyclodiene resistance (referred to here as Rdl^R). Previous work has shown that this alanine-serine substitution has a very small effect on the channel conductance of *Rdl*-containing receptors in *Drosophila* neurons (Zhang et al., 1994). The present study has shown similarly small conductance changes in *Rdl* homomultimers expressed in *Xenopus* oocytes (see Figs. 2 *A* and 3 *A*). Single base-pair substitutions were introduced into the *Rdl* cDNA via PCR mediated site-directed mutagenesis, as described by Landt et al. (1990), with modifications suggested by Kuipers et al. (1991). Mutations were introduced at position 319 into either the Rdl^S or Rdl^R cDNA. Asparagine 319 (N319) was selected for mutation because, as noted in the Introduction, this residue is adjacent to the site homologous to the extracellular ring of the nicotinic receptor, where most vertebrate $GABA_A$ receptor subunits have the basic amino acid arginine (Fig. 1). mRNA was synthesized from the Sp6 promoter in these constructs.

Oocyte expression

Xenopus laevis oocytes were prepared and injected with *Rdl* mRNAs as described previously (Zhang et al., 1995). Oocytes were maintained at 18°C for 1–13 days and prepared for single-channel recording by removal of the vitelline membrane (Stühmer, 1992).

Electrophysiology

Single-channel currents were recorded at room temperature in outside-out patches excised from oocytes. Patch electrodes were fabricated from borosilicate glass capillaries (i.d. 1.10 mm, o.d. 1.70 mm; Garner Glass Co., Claremont, CA), coated with Sylgard (Dow Corning, Midland, MI), and filled with the various pipette solutions (as indicated below). Patch electrodes had resistances of ~2–6 MΩ before seal formation. Outside-out patches were voltage-clamped, and currents were recorded with an EPC-7 patch-clamp amplifier (Instrutech, Elmont, NY). Signals were lowpass filtered at 1 kHz with an 8-pole Bessel filter (Frequency Devices, Haverhill, MA) and digitized at 2 kHz with a TL-1 DMA interface (Axon Instruments, Foster City, CA). Voltage was corrected for the liquid junction potential of each set of solutions (Neher, 1992). During recording, the oocytes were bathed in either *Drosophila* physiological saline (128 mM NaCl, 2 mM KCl, 4 mM $MgCl_2$, 1.8 mM $CaCl_2$, 35.5 mM sucrose, 5 mM HEPES, pH 7.1 titrated with NaOH) or in other solutions, as indicated in the figure legends. GABA (50 μM) was dissolved in bathing solution and applied in pulses of 200 ms with a Picospritzer (General Valve Corporation, Fairfield, NJ) from a 1–2-μm tipped pipette positioned near the patch. Patch pipettes were filled with 140 mM KCl, 10 mM HEPES, 10 mM EGTA, and 4 mM Mg-ATP, pH 7.1, or with other solutions, as indicated in the figure legends. Data were recorded with the computer program CLAMPEX (Axon Instruments).

Data analysis

Single-channel current records were analyzed with the computer program CLAMPFIT (Axon Instruments) to obtain average single-channel current amplitudes for a given voltage. Current-voltage plots were fitted to lines with the computer program ORIGIN (Mathcal, Northampton, MA). All measurements of single-channel conductance were taken from linear fits. Complete current-voltage plots were fitted to single lines or to separate lines for inward and outward currents. When the two separate fits had higher linear regression coefficients, these separate conductance values were presented. In most cases separate linear fits to inward and outward current did not change the estimates of reversal potential, but the reversal potentials for inward and outward currents sometimes differed by ~5 mV, and in these cases we used the mean of the two extrapolated intercepts. In a few instances where even the bilinear fits were poor, we fitted the current-voltage plot to the Goldman-Hodgkin-Katz (GHK) current equation. (It is important to state that this was done solely to provide an accurate estimate of the reversal potential from curved current-voltage plots. As indicated in the Results, this channel clearly violated the assumption of independence, so a fit to the GHK current equation has little physical meaning). The fitting methods for each experiment are mentioned in the figure legends or the text of the Results. Conductances and reversal potentials from different patches were averaged and presented as mean ± standard error.

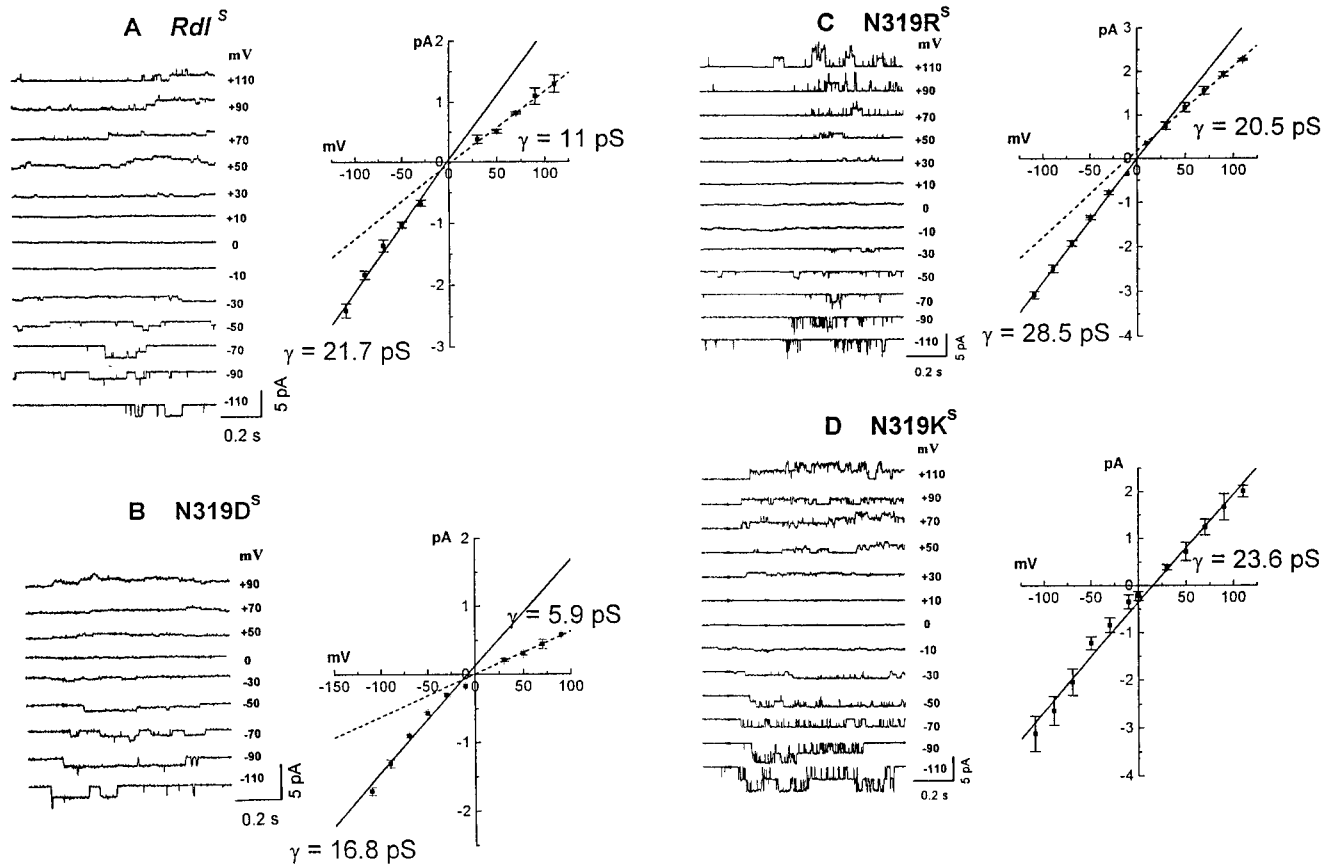

FIGURE 2 Single-channel currents and current-voltage plots for *Drosophila Rdl*^{S} channels (*A*), N319D^S mutant channels (*B*), N319R^S mutant channels (*C*), and N319K^S mutant channels (*D*). Holding potentials are indicated to the right of the single-channel traces. The solutions were those given in Materials and Methods. Conductances shown were mean values (see text). Note the rightward shift in reversal potential to 15.9 mV in the N319K^S mutant channel in *D*.

Reversal potentials (E_{rev}) from current-voltage plots were used to calculate the permeability ratio of ion X to Cl^-, P_X/P_{Cl}, according to the GHK voltage equation:

$$E_{rev} = \frac{RT}{zF} \ln\left(\frac{a_{Cl_i} + a_{X_o}P_X/P_{Cl}}{a_{Cl_o} + a_{X_i}P_X/P_{Cl}}\right)$$

a represents the activity of the species indicated by the subscript, and *R*, *T*, *z*, and *F* have their usual meanings. Throughout this analysis ion activities were used instead of ion concentrations, with coefficients computed from the tables of Robinson and Stokes (1959). The subscripts o and i denote external and internal, respectively, where external means the bathing solution and internal means the solution in the patch pipette. For outside-out patches, this corresponds to the solutions at the extracellular and intracellular faces of the membrane, respectively. When species X was an anion (e.g., acetate), a_{Xo} and a_{Xi} in the above equation were exchanged.

RESULTS

Charge effects

To test for the role of electrical charge, we replaced the neutral polar asparagine at position 319 with both acidic and basic amino acids. Single-channel current traces and current-voltage plots are shown for the cyclodiene-sensitive *Rdl*^{S} channel (Fig. 2 *A*) and for mutant channels prepared on the cyclodiene-sensitive background. The mutant channels have aspartate (N319D^S, Fig. 2 *B*), arginine (N319R^S, Fig. 2 *C*), and lysine (N319K^S, Fig. 2 *D*) replacing N319. Data are also shown for cyclodiene-resistant *Rdl*^{R} channels (Fig. 3 *A*) and for a mutant channel prepared on the cyclodiene-resistant background with a lysine replacement (N319K^R, Fig. 3 *B*). *Rdl*^{S} and *Rdl*^{R} receptors had similar single-channel current-voltage plots, as noted previously in *Drosophila* neurons (Zhang et al., 1994). Furthermore, as with wild type, no subconductance states were seen in the mutant channels studied here. Therefore, plots of single-channel current versus voltage gave the conductance for the main conductance state of the channel. No significant differences were found between the sensitive and resistant variants in conductances for either outward or inward current (*Rdl*^{S}, inward conductance: 21.7 ± 1.0 pS, $n = 10$; outward conductance: 11.0 ± 2.0 pS, $n = 7$; *Rdl*^{R}, inward conductance: 19.1 ± 1.1 pS, $n = 8$; outward conductance: 9.6 ± 0.5 pS, $n = 8$). The difference between conductances for inward and outward current reflects a rectification property intrinsic to this channel (Zhang et al., 1994, 1995). Alterations in this property by mutations will be noted shortly below.

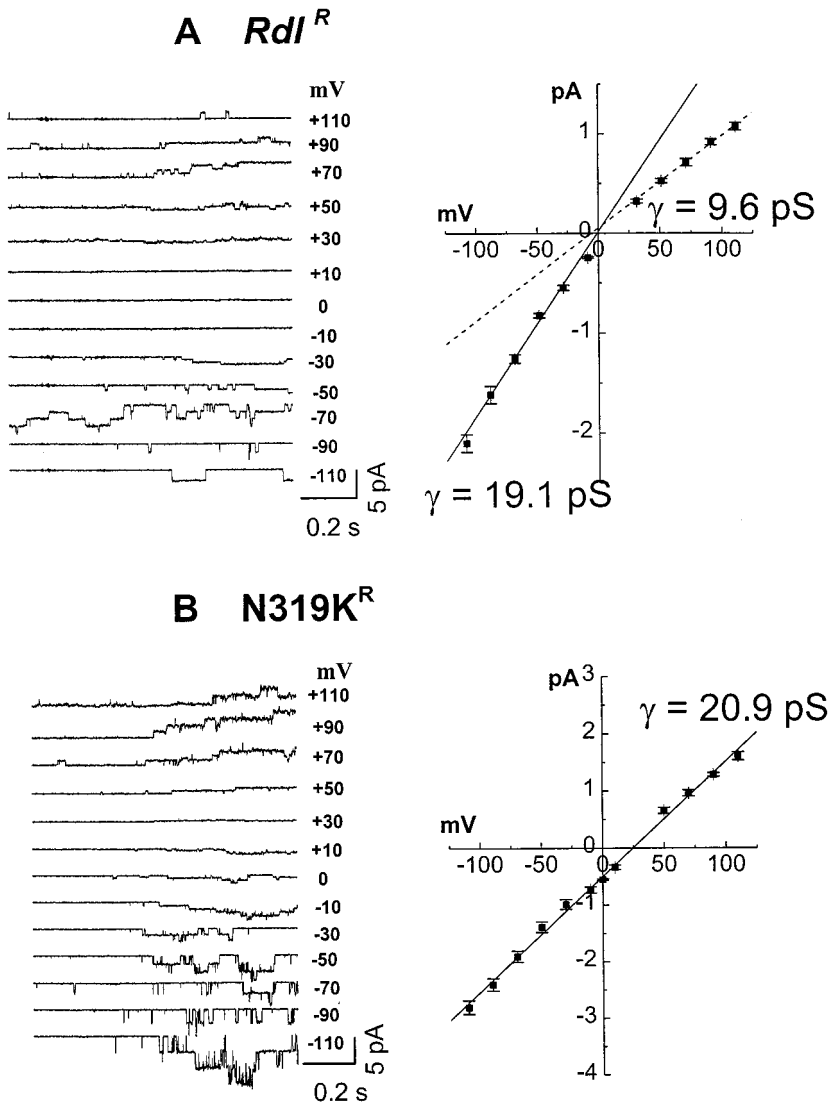

FIGURE 3 Single-channel currents and current-voltage plots for the *Drosophila Rdl*^{R} channels (*A*) and N319K^R mutant channels (*B*). The bathing and pipette solutions were the same as in Fig. 2. Note the rightward shift in reversal potential to 24.7 mV for the N319K^R mutant channel in *B* (see also Fig. 2 *D*).

The negative charge mutation, N319D^S, lowered the conductance for inward and outward current to 16.8 ± 0.6 pS and 5.9 ± 1.3 pS (n = 7), respectively (on the *Rdl*^{S} background). The positive charge mutation, N319R^S, increased the conductance of both inward and outward current to 28.5 ± 0.9 pS (n = 9), and 20.5 ± 2.0 pS (n = 5), respectively (again on the *Rdl*^{S} background). These results are consistent with a simple electrostatic interaction between permeating anions and charge at this site.

Replacing N319 with another positively charged amino acid, lysine, also increased the single-channel conductance in both the *Rdl*^{S} and *Rdl*^{R} backgrounds (Figs. 2 *D* and 3 *B*). However, this mutation also removed the rectification to produce linear current-voltage plots with conductances of 23.6 ± 0.8 pS for N319K^S (n = 9) and 20.9 ± 0.4 pS for N319K^R (n = 14). All of the other channels discussed above showed rectification, including the channel with arginine at residue 319. Thus the loss of rectification in N319K channels cannot be explained as a consequence of charge.

Figs. 2 *D* and 3 *B* show a particularly striking consequence of lysine substitution at residue 319: the reversal potential was shifted in the positive direction. Even though these recordings were made in essentially symmetrical Cl^- (140 mM internal [Cl^-] and 141.6 mM external [Cl^-]), the reversal potentials were 15.9 ± 2.5 mV (n = 9) for N319K^S (Fig. 2 *D*) and 24.7 ± 2.3 mV (n = 12) for N319K^R (Fig. 3 *B*). Note that a negative single-channel current was seen at +10 mV for the N319K^R channel, indicating that it reverses well above zero. Furthermore, when a voltage ramp was applied, the open channel current of N319K^R reversed at 23.7 mV. All of the four other channels examined above under these same conditions had reversal potentials near zero. Because there were no significant osmotic gradients, we cannot account for this large positive reversal potential shift with streaming potentials or dilution potentials. This result therefore suggests that the replacement of asparagine 319 with lysine makes the channel permeable to other ions besides Cl^-.

Cation permeation of N319K channels

Cation permeability was the most likely explanation for the positive reversal potential of the two N319K mutants shown in Figs. 2 *D* and 3 *B*, because cations were asymmetrically distributed in these experiments. The principal cation of the external solution was Na^+, and the principal cation of the internal solution was K^+. We therefore tested the effects of changes in cations, and because the reversal potential shift was greater in $N319K^R$ compared to $N319K^S$, we used the $N319K^R$ mutant channel (lysine replacement at residue 319 on a cyclodiene-resistant background) for further study. First we examined the current-voltage behavior of this channel in nearly symmetrical NaCl, with 135 mM internal and 150 mM external Na^+ (pH adjustment was made with NaOH; intracellular and extracellular [Cl^-] were 140 mM and 141.6 mM, respectively). Under these essentially symmetrical conditions the current-voltage plot for the $N319K^R$ mutant channel reversed near zero (1.9 ± 0.4 mV, $n = 10$) (Fig. 4, *triangles*), and the single-channel conductance remained essentially the same (21.4 ± 0.4 pS, $n = 11$; Fig. 4, *triangles*) compared with that in the original NaCl/KCl solutions (Fig. 4, *squares*, same as Fig. 3 *B*). Reversing the NaCl/KCl to the opposite sides of the membrane from that used in Fig. 3 *B* moved the reversal potential to the opposite side of the current axis (Fig. 4, *circles*), again leaving the channel conductance almost unchanged at 19.0 ± 0.5 pS ($n = 4$). However, the reversal potential shift in the negative direction of −14.8 ± 0.6 mV ($n = 4$) was smaller than the value of 24.7 mV in the positive direction, indicating that cation gradients have an asymmetrical effect on the reversal potential of this channel.

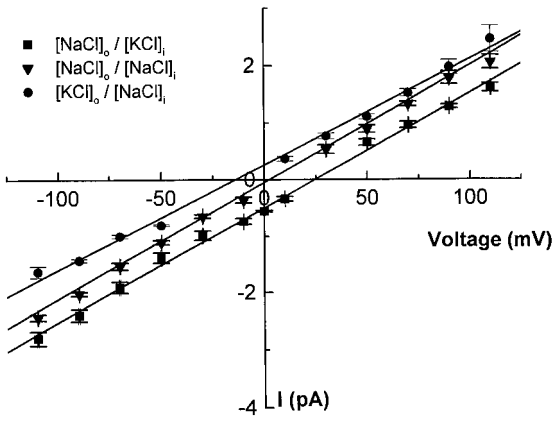

FIGURE 4 Effects of cation asymmetry on the reversal potentials of $N319K^R$ mutant channels. Current-voltage plots were obtained from recordings in external NaCl/internal KCl (■), external NaCl/internal NaCl (▼), and external KCl/internal NaCl (●). For external NaCl/internal KCl, the solutions are those stated in Materials and Methods (note that this is the same plot as in Fig. 3 *B*). For external NaCl/internal NaCl the same solutions were used, except that 140 mM NaCl replaced KCl in the pipette. For external KCl/internal NaCl, outside-out patches were formed with an exact reversal of the solutions used in the external NaCl/internal KCl current-voltage plot. Thus, in this experiment the patch pipette contained *Drosophila* physiological saline, and the bath contained the patch pipette solution given in Materials and Methods.

Fig. 4 shows that the reversal potential of the $N319K^R$ mutant channel is sensitive to the distribution of cations between the external and internal solutions, thus indicating that the $N319K^R$ mutant channel is cation permeable. Furthermore, these results indicate that this channel has a greater permeability for Na^+ than for K^+, because if the permeabilities for these two ions were equal, the reversal potential would have remained at zero. In comparing the different current-voltage plots in Fig. 4, it is notable that the channel conductance remained the same. Because the permeability for Na^+ must be greater than that for K^+ (to give the nonzero reversal potentials observed), greater currents would be expected when the membrane potential favors Na^+ current rather than K^+ current. This finding of similar conductances but different permeabilities is the first of a number of results presented here that indicate that ion fluxes are not independent in this channel.

To quantify the cation permeability in the $N319K^R$ mutant channel, we determined the permeability ratio of K^+ to Cl^- by holding external [KCl] fixed, while varying internal [KCl] and maintaining osmolarity with sucrose. Reducing internal [KCl] to 20 mM moved the reversal potential of the $N319R^S$ channel to −43.7 mV (Fig. 5 *A*). For the same solutions, the $N319K^R$ channel reversed at −20.2 mV (Fig. 5 *B*). The reversal potentials are different from the Cl^- Nernst potential (−47.1 mV), and these differences can be attributed to K^+ permeability. For the $N319K^R$ channel, the plot of reversal potential versus pipette KCl activity obeyed the GHK voltage equation, with $P_K/P_{Cl} = 0.33$ (Fig. 6, *dotted curve*). The reversal potential measurements for Rdl^S, Rdl^R, and $N319R^S$ indicated that P_K/P_{Cl} ratios of these channels were all very small. For $N319R^S$ channels the value was 0.013, and for the two other channels the ratio was indistinguishable from zero. The solid line in Fig. 6 shows the expected behavior of a channel permeable only to Cl^-; the points for the two wild-type channels, Rdl^S and Rdl^R, and the mutant $N319R^S$ channel are very close to this line. These results confirm the suggestion based on the results in Fig. 4 that substitution of a lysine at residue 319 increases the cation permeability of the channel.

Finally, we note another observation that indicates that the fluxes of different ions are not independent. The current voltage plot in a KCl gradient is essentially linear (Fig. 5 *B*), with equal slopes for inward and outward current (16.0 ± 1.1 pS, $n = 12$). However, outward current should be greater than inward current because outward current is carried by more permeable Cl^-, but inward current should reflect movement of less permeable K^+. The linear behavior observed in Fig. 5 *B* can thus be interpreted as evidence against the hypothesis that K^+ flux and Cl^- flux are independent.

Cation and anion interactions

To test the interdependence of Cl^- and K^+ permeation more explicitly, we replaced each of these ions in turn with large organic ions that should permeate the channel poorly. When

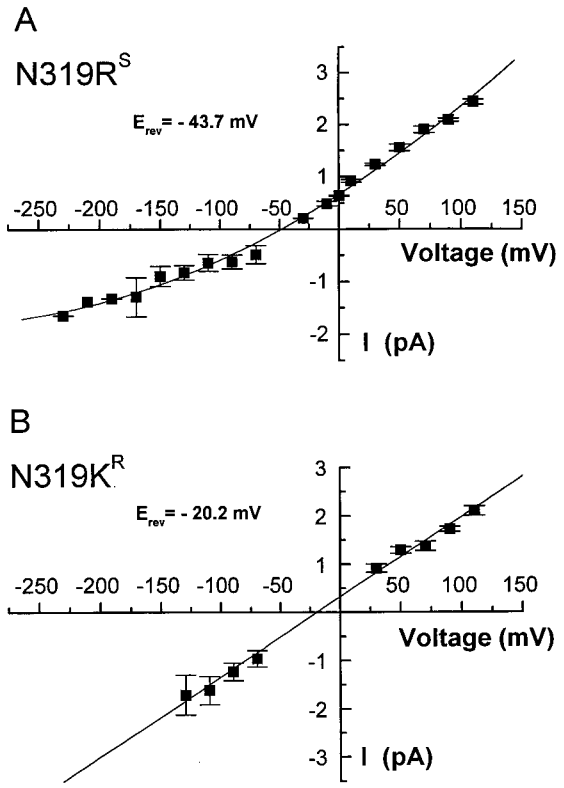

FIGURE 5 Potassium permeability measurement. Current-voltage plots were obtained from the N319R^S (n = 5) and N319K^R (n = 12) mutant channels. (*A*) For the N319R^S mutant channels, the reversal potential was −43.7 mV. The reversal potential was estimated by fitting the Goldman-Hodgkin-Katz current equation. This value of the reversal potential yielded P_K/P_{Cl} = 0.013. (*B*) For the N319K^R mutant channel, the reversal potential obtained by linear fit was −20.2 ± 8.3 mV, giving P_K/P_{Cl} = 0.34. The bathing solution contained 130 mM KCl, 4 mM $MgCl_2$, 1.8 mM $CaCl_2$, 35.5 mM sucrose, and 5 mM HEPES (pH 7.1); the pipette solution contained 20 mM KCl, 240 mM sucrose, 10 mM HEPES, 10 mM EGTA, and 4 mM ATP (pH 7.1).

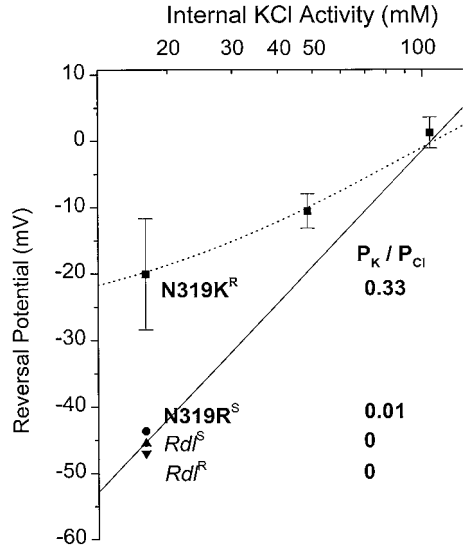

FIGURE 6 Reversal potential versus internal KCl activity. Reversal potentials and permeability ratios (P_K/P_{Cl}) were obtained for the *Rdl*^{S} (▲; n = 10), *Rdl*^{R} (▼; n = 5), N319R^S (●; n = 5), and N319K^R (■; for 20 mM KCl, n = 12; for 60 mM KCl, n = 9; for 140 mM KCl, n = 10). The reversal potentials for N319K^R were obtained from current-voltage plots by linear fitting. For the N319K^R mutant channels, fitting the plot of reversal potential versus KCl activity to the GHK voltage equation (see Materials and Methods) gave P_K/P_{Cl} = 0.33 (· · · ·). With the solutions used for the experiments in Fig. 5, the reversal potentials were −43.7 mV for N319R^S, −45.5 mV for *Rdl*^{S}, and −47.0 mV for *Rdl*^{R} (estimated by fitting current-voltage plots to the GHK current equation). These gave P_K/P_{Cl} = 0.013 for N319R^S and values indistinguishable from zero for *Rdl*^{S} and *Rdl*^{R}. The bathing solution was 130 mM KCl, 4 mM $MgCl_2$, 1.8 mM $CaCl_2$, 35.5 mM sucrose, and 5 mM HEPES (pH 7.1). The pipette contained various KCl concentrations (converted to activity for the x axis), with replacement by sucrose. The other components of the pipette solution were 10 mM HEPES, 10 mM EGTA, and 4 mM Mg-ATP, pH 7.1.

Cl^- on the intracellular side was replaced by gluconate, inward channel current could no longer be seen, even with voltages as negative as −180 mV (n = 10). This indicates that very little K^+ can flow from the outside to the inside without Cl^- on the inside (Fig. 7, *triangles*). The channel conductance of 10.8 ± 0.5 pS (n = 10) was about half that seen in symmetrical KCl (19.7 ± 0.2 pS, n = 7). Thus even Cl^- flow from the outside to the inside was influenced by Cl^- on the intracellular side. The extrapolated reversal potential of this plot was −113 ± 3.8 mV (n = 9), which with the aid of the GHK voltage equation gave P_K/P_{Cl} = 0.012. This value differs dramatically from the value of 0.33 determined above (Fig. 6). This result implies an interaction between permeating anions and cations, such that cation permeability is much higher in the presence of permeable anions.

When K^+ on the intracellular side was replaced by the large organic cation *N*-methylglucamine (NMG), the result was far less dramatic. Both inward and outward currents were clearly observed (Fig. 7, *squares*), and the single-channel conductance remained essentially the same (20.3 ± 1.1 pS; n = 5). Thus Cl^- movement shows no discernible dependence on cations. The similar conductances in solu-

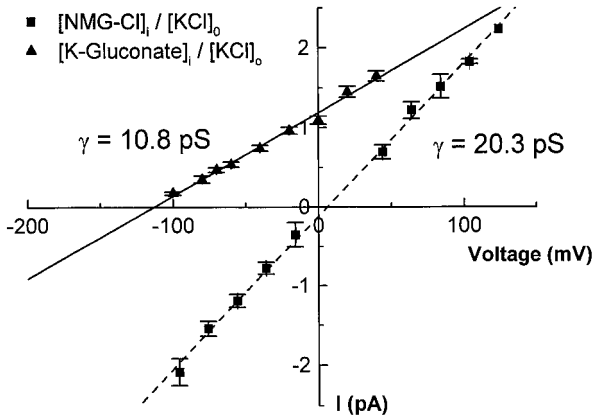

FIGURE 7 Effects of large organic cations and anions on the conductance and reversal potential of the N319K^R mutant channel. Current-voltage plots are shown for *N*-methyl-glucamine substitution for K^+ (■) and gluconate substitution for Cl^- (▲) in the pipette solutions used for the experiments in Fig. 2. The bathing solution was the same as in Fig. 5.

tions with and without permeating cations suggest that the permeation of cations makes little contribution to the single-channel current. Thus, as suggested by the similar slopes in Fig. 4, cations permeate the N319K^R channel but carry little if any current. This situation is similar to that described by Franciolini and Nonner (1987, 1994a,b) in the hippocampal Cl^- channel (see Discussion).

The positive reversal potential in the NMG/Cl^- plot of Fig. 7 is consistent with the experiments in Fig. 6 dealing with K^+ permeability. Using the GHK voltage equation, with a measured reversal potential of 5.9 ± 2.4 mV (n = 5), and assuming zero permeability for NMG, we calculated P_K/P_{Cl} = 0.29, which was close to the value of 0.33 from Fig. 6. Note that if we use P_K/P_{Cl} = 0.33 from the experiment in Fig. 6, then the reversal potential of 5.9 mV in the internal NMG-Cl/external KCl solutions gives a value for P_{NMG}/P_{Cl} of 0.03. Thus a low NMG permeability is consistent with our earlier measurements of P_K/P_{Cl}, justifying our use of this substance as an impermeable substitute for inorganic cations.

Organic anion permeability

To explore the possibility that changes in pore size are associated with the changes in permeation properties, we determined the permeability ratios for formate, acetate, and propionate relative to Cl^-. These organic anions provide a series of increasing sizes, with Stokes diameters of 3.37 Å for formate, 4.49 Å for acetate, and 5.13 Å for propionate (computed from the limiting ion conductivities of Robinson and Stokes (1959)). The decrease in permeability with anion size was used previously to estimate the size of the pore in vertebrate $GABA_A$ receptor channels (Bormann et al., 1987). Solutions with internal organic anions and external Cl^- were used to measure reversal potential shifts, allowing us to obtain P_X/P_{Cl} from the GHK voltage equation. Both internal and external solutions contained NMG as the cation to avoid the contribution of cation permeability to reversal potential. The current-voltage plots for acetate are shown in Fig. 8 for *Rdl*^{S}, *Rdl*^{R}, and N319K^R. The reversal potentials were −78.6 ± 6.0 mV for *Rdl*^{S} (n = 5), −76.0 ± 2.9 mV for *Rdl*^{R} (n = 8), and −68.2 ± 2.2 mV for the N319K^R mutant (n = 8). The value for N319K^R was significantly different from that for *Rdl*^{R} ($p < 0.05$), but not from that for *Rdl*^{S} (p = 0.08). From these reversal potentials we obtained P_{Ac}/P_{Cl} values of 0.049 for *Rdl*^{S}, 0.047 for *Rdl*^{R}, and 0.064 for N319K^R.

The permeability ratios were determined for formate and propionate as well (in *Rdl*^{R} and N319K^R), and the values are plotted versus the Stokes diameter (Fig. 9). This plot shows the expected trend of decreasing permeability with anion size. These data were fitted to the models used by Dwyer et al. (1980) and Bormann et al. (1987). Although these models failed to account quantitatively for the size dependence, the fits gave pore sizes in the 5–6 Å range, and the pore size of N319K^R was 0.3 Å larger in each case. Our data show an exponential decrease in P_X/P_{Cl} with size. The physical significance of such a dependence is not clear, other than possibly as a Boltzmann term with a size-dependent energy

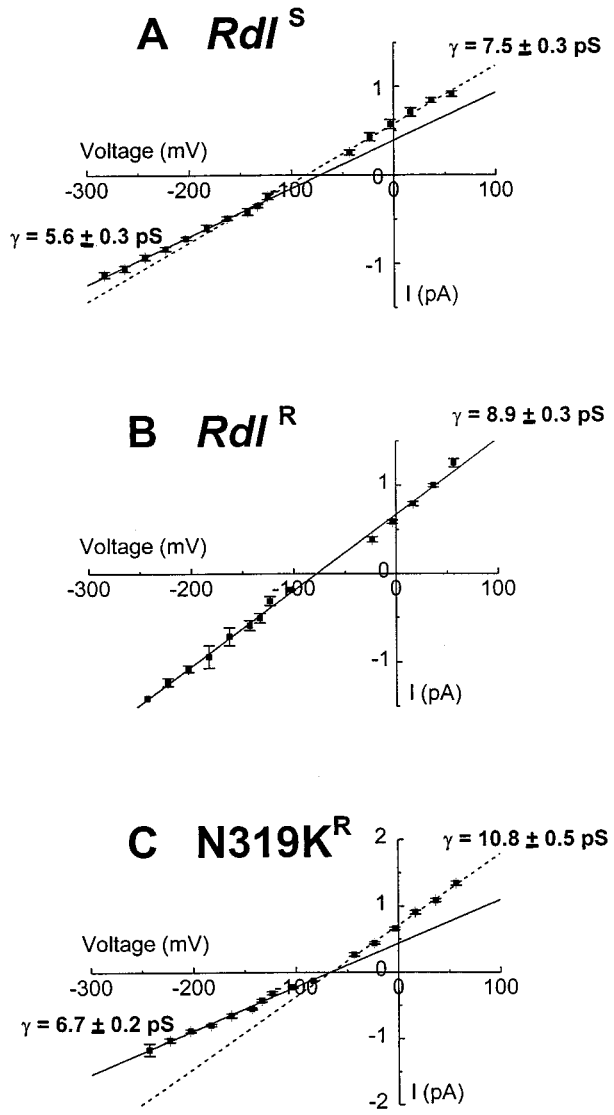

FIGURE 8 Acetate permeation. Current-voltage plots in *Rdl*^{S} (*A*), *Rdl*^{R} (*B*), and N319K^R mutant (*C*) channels. The pipette contained 140 mM *N*-methyl-glucamine acetate, 10 mM HEPES, 10 mM EGTA, and 4 mM Mg-ATP (pH 7.1); the bathing solution contained 130 mM *N*-methyl-glucamine chloride, 4 mM $MgCl_2$, 1.8 mM $CaCl_2$, 35.5 mM sucrose, and 5 mM HEPES (pH 7.1). (*A*) Current was averaged from eight patches for inward current and five for outward current. The plot in *A* exhibited rectification, with inward and outward currents extrapolating to −78.6 ± 6.8 mV and −74.3 ± 3.2 mV, respectively. For the five patches with both inward and outward currents, the average reversal potential was −78.6 ± 6.0 mV (n = 5), used for subsequent permeability ratio calculation. (*B*) Current was averaged from eight patches. The average reversal potential was −76.0 ± 2.9 mV from a linear fit. (*C*) Current was averaged from eight patches for inward current and 10 patches for outward current. The channel in *C* also exhibited slight rectification, giving extrapolated reversal potentials of −70.9 ± 2.3 mV for inward current and −65.6 ± 2.8 mV for outward current. The average was −68.2 ± 2.2 (n = 8) mV. The conductances shown were obtained as separate slopes for inward and outward currents in *A* and *C*. Conductances were averaged after determination from each separate patch.

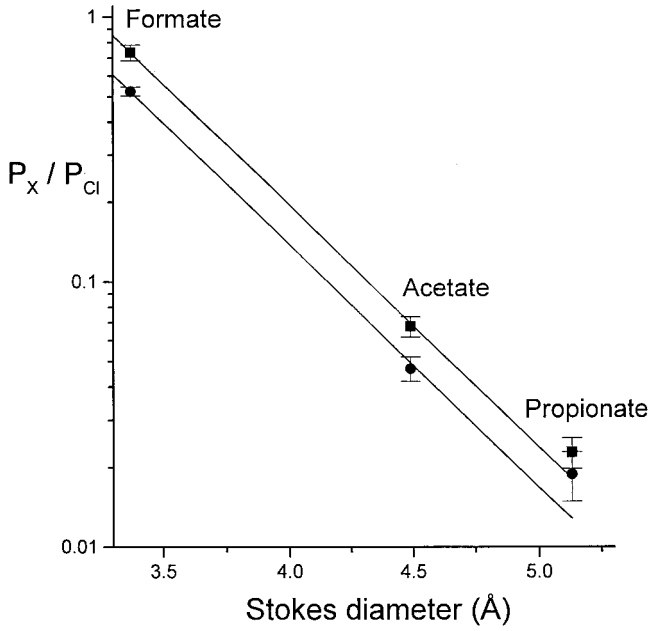

FIGURE 9 Plot of permeability ratio versus Stokes diameter. Permeability ratios for formate, acetate, and propionate were determined from reversal potentials, using solutions as in Fig. 8, with different organic anions in the pipette solution. Squares are for N319K^R and circles are for *Rdl*^{R}. Each point reflects 4–12 experiments. The best fitting exponential functions are drawn through the data points and suggest that the N319K^R channel has a pore that is 0.2 Å larger than the pore of the *Rdl*^{R} channel (see text). The differences are statistically significant for formate and acetate ($p < 0.05$).

of ions penetrating the channel. The plot for N319K^R and the best fitting exponential functions are shifted to the right by ~0.2 Å relative to the plot for *Rdl*^{R}. Thus, depending on choice of model, these results suggest that the mutation of N to K at position 319 increases the pore size by 0.2–0.3 Å.

Under the conditions of these experiments, inward current was carried by organic anion from the internal solution, and outward current was carried by Cl^- from the external solution. Thus it is surprising that in all three channels the putative acetate conductances are similar to or only slightly less than the Cl^- conductances (Fig. 8). Because the reversal potentials indicate that acetate is 15- to 21-fold less permeable than Cl^-, it would appear once again that permeability and conductance are not related in a simple way, providing yet another example of violation of the independence of ion fluxes. This view is underscored by the comparison of conductances between *Rdl*^{R} and N319K^R in acetate. The conductance for inward current (carried by acetate) in the N319K^R channel is lower than that in the *Rdl*^{R} channel, but the permeability ratio for acetate to Cl^- in the N319K^R channel is higher. This trend did not extend to propionate. The single-channel currents were very small when current was carried by this larger anion and often could not be seen at all, even with voltages of −230 mV. From experiments where the noise was low enough to see inward currents (<0.3 pA in amplitude at −200 mV), the conductances for apparent propionate fluxes were 2.9 ± 0.8 pS ($n = 4$) for *Rdl*^{R} and 2.8 ± 0.4 pS ($n = 3$) for N319K^R. However, the conductance was also reduced for current carried by Cl^- in the opposite direction (11.2 ± 0.7 pS for N319K^R, $n = 11$; and 7.0 ± 0.5 pS for *Rdl*^{R}, $n = 7$), and this is yet another result that suggests interactions between ion fluxes.

DISCUSSION

Electrostatic effects on permeation

The initial goal of this study was to explore the role of electrostatic interactions between permeating ions and residue 319 in the *Drosophila Rdl* GABA receptor. Some of our results are in fact consistent with such an interaction. The wild-type receptor has the neutral polar amino acid asparagine at this position. When it was replaced by aspartate, the conductance for both inward and outward current went down, and when it was replaced by arginine both conductances went up. Presumably the receptor encoded by the *Rdl* gene is composed of five identical subunits, in keeping with the pseudo-fivefold symmetry suggested for $GABA_A$ receptors (Nayeem et al., 1994) and nicotinic receptors (Karlin and Akabas, 1995). This means that single charge replacements should be multiplied by five when one considers the total change in charge at a putative ring formed by all five subunits. In the nicotinic receptor, five charge replacements in the extracellular ring (one residue away from N319; Fig. 1) reduced the conductance by fourfold (Imoto et al., 1988). Compared to this, the changes described in the present study are rather small (Fig. 2). However, the residue homologous to N319 in $GABA_A$ receptors was inaccessible to cysteine scanning and is therefore buried within the protein (Xu and Akabas, 1996). This would place this residue at a greater distance from the aqueous permeation pathway and explain the weaker interaction. These are the only results we obtained that fit with an electrostatic interaction. The results discussed below indicate different forms of interactions and require an explanation in terms of fundamentally different mechanisms.

Conformational effects on permeation

The following results cannot be explained in terms of electrostatic interactions. The lysine-substituted mutant channels, N319K^S and N319K^R are permeable to cations. Both lysine and arginine carry a single positive charge in solution at neutral pH, so the changes caused by exchange of these two amino acids are not likely to be electrostatic. Furthermore, although the cation permeability caused by the exchange of arginine and lysine is surprising, it is paradoxical in view of the cation impermeability of the asparagine (wild-type) and aspartate-containing channels. Adding positive charge should reduce cation permeability, not increase it. The appearance of cation permeability is accompanied by a striking interdependence of ion fluxes. The possible permeation of the N319K^R channel by multiion complexes

(discussed below), together with the cation permeability, suggests that this mutation alters the underlying mechanism of ion permeation in a fundamental way. Because these changes go well beyond what can be expected from a simple change in charge, it is likely that lysine substitution at this site induces a change in the conformation of the protein, such that the positions of other residues are altered. Further evidence for a conformational effect comes from considering the result that lysine substitution at position 319 increased the permeability to organic anions, because this indicates an increase in the size of the pore. The size filter in the nicotinic receptor is thought to be quite distant from the extracellular ring, in the lower M2 region near the intermediate ring of charge (Villarroel et al., 1991). Thus the apparent size change also requires an action at a distance through a change in the conformation of the protein. This conformational change would then emanate from residue 319 and extend to the deeply situated selectivity filter of the channel.

It has been pointed out that conductance mutations near this location in nicotinic receptors failed to show the ionic strength dependence expected for a simple electrostatic mechanism, and global structural changes were among the alternative explanations considered (Kienker et al., 1994). An especially interesting comparison can be made with the results of Galzi et al. (1992), who found that insertion of a proline before ring 2 in the nicotinic receptor α_7 subunit (where a gap appears in the alignment with the GABA receptors in Fig. 1) renders the channel anion permeable. This result was also interpreted in terms of a structural realignment of the M2 segment, but in this case it was initiated at the opposite end. The fact that such conformational changes influence anion-cation selectivity lends support to the speculative idea that hydroxyl side chains can serve as "ambidextrous" ligands. Depending on the specific three-dimensional arrangement of side chains and backbone carbonyls, a channel could interact preferentially with either anions or cations or both (Eisenman and Alvarez, 1991).

Cysteine-scanning studies have shown that the residue homologous to N319 in vertebrate $GABA_A$ receptors is inaccessible to sulfhydryl reagents and is presumably embedded within the protein (Xu and Akabas, 1996). Thus it is likely that this residue plays a structural role in anchoring the C-terminal part of the M2 segment. A lysine substitution could then alter the interaction with other domains to shift the position of the entire M2 segment. In this way the amino acid in the distant residue 302 (the site that determines cyclodiene sensitivity) could change its position to allow the N319K mutation to have different consequences in the cyclodiene-resistant and -sensitive backgrounds, as observed (Fig. 2 *D* versus Fig. 3 *B*). Alternatively, the tendency for the M2 segment to adopt an α-helical conformation in the *Rdl* GABA receptor may be sensitive to the amino acid in position 319. In synthetic peptides, arginine-lysine substitutions were shown to have long-range effects on the tendency to form α-helices versus 3_{10}-helices (Fiori et al., 1994), so similar long-range effects in the GABA receptor protein are a possibility.

The hippocampal chloride channel and multiion permeation

Some of the permeation properties of the $N319K^R$ channel described here resemble those of a rat hippocampal voltage-dependent Cl^- channel, studied in detail by Franciolini and Nonner (1987, 1994a,b). We note the following two similarities: 1) The two channels are cation permeable in similar ratios: 0.2 for the hippocampal Cl^- channel and 0.33 here. 2) In the absence of anions, permeation by cations is not detectable. We also note two differences: 1) The $N319K^R$ channel shows a strong preference for Na^+ over K^+, but the hippocampal Cl^- channel has equal permeabilities for these two cations. 2) The hippocampal Cl^- channel has higher permeability for the organic anion acetate ($P_{Ac}/P_{Cl} = 0.66$) than the $N319K^R$ channel ($P_{Ac}/P_{Cl} = 0.064$), implying that the hippocampal Cl^- channel has a larger pore diameter. More generally, in both channels ion fluxes appear to be interdependent. The properties of the hippocampal Cl^- channel have been explained by models involving ion complexes as permeating species (Franciolini and Nonner, 1994b). Thus it is possible that some of the results seen in the $N319K^R$ channel can be explained by a similar mechanism. A large number of results in this study were noted that were inconsistent with the GHK equation and thus suggest that ion fluxes are not independent. These results may be an indication of permeation by ionic complexes, as proposed by Franciolini and Nonner, or alternatively, the inadequacy of the GHK equation may reflect a more complicated dependence of permeability ratios on ion composition.

Reversal potentials of GABA-gated channels

The reversal potentials of $GABA_A$ receptor channels show considerable variation between different vertebrate preparations. Even at different locations in the same cell, GABA can either depolarize of hyperpolarize, despite the fact that a Cl^--selective channel is activated at both sites (Alger, 1985). The mechanisms of these actions in some cases have been attributed to differences in intracellular [Cl^-] (Zhang and Jackson, 1993), as well as to shifts in the transmembrane bicarbonate gradient (Staley et al., 1995). Vertebrate $GABA_A$ receptors exhibit enormous molecular diversity (Luddens and Wisden, 1991; Whiting et al., 1995). Although no $GABA_A$ receptor subunit contains a lysine at the residue homologous to N319 of the *Rdl* gene product, lysine is occasionally found at the adjacent position, i.e., in the extracellular ring. If some $GABA_A$ receptor variants have channels that allow ions to permeate by a mechanism similar to that found for the $N319K^R$ channel, then the Na^+ and K^+ gradients of a cell would lead to reversal potentials that are positive relative to the Nernst potential for Cl^-. This provides a new hypothesis for the diversity of neuronal

responses to GABA, namely that a $GABA_A$ receptor has *Rdl* N319K-like behavior, so that its reversal potential is determined by cations as well as anions.

CONCLUSIONS

These studies showed that a residue of the *Drosophila Rdl* GABA receptor channel adjacent to the extracellular ring of negative charge in nicotinic receptors influences ion permeation by both electrostatic and nonelectrostatic mechanisms. Because the changes in permeation properties resulting from mutations at this site were extensive and were associated with an increase in pore size, we were led to propose a change in protein conformation. These results suggest that the arrangement of the peptide chains can determine the anion-cation selectivity of a channel. This point has been made on the basis of very different mutations in nicotinic receptors (Galzi et al., 1992) and is relevant to the question of how channels with both anion and cation selectivity evolved within the same gene superfamily.

We thank Drew Boileau and Cindy Czajkowski for the pile-up of aligned sequences used to interpret our results, and Gail Robertson for providing facilities for oocyte expression.

This research was supported by National Institutes of Health grant NS23512.

REFERENCES

Alger, B. E. 1985. GABA and glycine: postsynaptic actions. *In* Neurotransmitter Actions in the Vertebrate Nervous System. Plenum, New York.

Bormann, J., O. P. Hamill, and B. Sakmann. 1987. Mechanism of anion permeation through channels gated by glycine and γ-aminobutyric acid in mouse cultured spinal neurones. *J. Physiol. (Lond.).* 385:243–286.

Dwyer, T. M., D. J. Adams, and B. Hille. 1980. The permeability of the endplate channel to organic cations in frog muscle. *J. Gen. Physiol.* 75:469–492.

Eisenman, G., and O. Alvarez. 1991. Structure and function of channels and channelogs as studied by computational chemistry. *J. Membr. Biol.* 119:109–132.

ffrench-Constant, R. H., D. P. Mortlock, C. D. Shafer, R. J. MacIntyre, and R. T. Roush. 1991. Molecular cloning and transformation of cyclodiene resistance in *Drosophila*: an invertebrate $GABA_A$ receptor locus. *Proc. Natl. Acad. Sci. USA.* 88:7209–7213.

ffrench-Constant, R. H., T. A. Rocheleau, J. C. Steichen, and A. E. Chalmers. 1993. A point mutation in a *Drosophila* GABA receptor confers insecticide resistance. *Nature.* 363:449–451.

Fiori, W. R., K. M. Lundberg, and G. L. Millhauser. 1994. A single carboxy-terminal arginine determines the amino-terminal helix conformation of an alanine-based peptide. *Nature Struct. Biol.* 1:374–377.

Franciolini, F., and W. Nonner. 1987. Anion and cation permeability of a chloride channel in rat hippocampus neurons. *J. Gen. Physiol.* 90: 453–478.

Franciolini, F., and W. Nonner. 1994a. Anion-cation interactions in the pore of neuronal background chloride channels. *J. Gen. Physiol.* 104: 711–723.

Franciolini, F., and W. Nonner. 1994b. A multi-ion permeation in neuronal background chloride channels. *J. Gen. Physiol.* 104:725–746.

Galzi, J. L., A. Devillers-Thiery, N. Hussy, S. Bertrand, J. P. Changeux, and D. Bertrand. 1992. Mutations in the channel domain of a neuronal nicotinic receptor convert ion selectivity from cationic to anionic. *Nature.* 359:500–505.

Imoto, K., C. Busch, B. Sakmann, M. Mishina, T. Konno, J. Nakai, H. Bujo, Y. Mori, K. Fukuda, and S. Numa. 1988. Rings of negatively charged amino acids determine the acetylcholine receptor channel conductance. *Nature.* 335:645–648.

Karlin, A., and M. H. Akabas. 1995. Toward a structural basis for the function of the nicotinic acetylcholine receptors and their cousins. *Neuron.* 15:1231–1244.

Kienker, P., G. Tomaselli, M. Jurman, and G. Yellen. 1994. Conductance mutations of the nicotinic acetylcholine receptor do not act by a simple electrostatic mechanism. *Biophys. J.* 66:325–334.

Kuipers, O. P., H. J. Boot, and W. M. de Vos. 1991. Improved site-directed mutagenesis method using PCR. *Nucleic Acids Res.* 19:4558.

Landt, O., H.-P. Grunert, and U. Hahn. 1990. A general method for rapid site directed mutagenesis using polymerase chain reaction. *Gene.* 96: 125–128.

Langosch, D., B. Laube, N. Rundström, V. Schmieden, J. Bormann, and H. Betz. 1994. Decreased agonist affinity and chloride conductance of mutant glycine receptors associated with human hereditary hyperekplexia. *EMBO J.* 13:4223–4228.

Lee, H.-J., T. Rocheleau, H.-G. Zhang, M. B. Jackson, and R. H. ffrench-Constant. 1993. Expression of a *Drosophila* GABA receptor in a baculovirus insect cell system: functional expression of insecticide susceptible and resistant GABA receptors from the cyclodiene resistance gene *Rdl. FEBS Lett.* 335:315–318.

Lester, H. A. 1992. The permeation pathway of neurotransmitter-gated ion channels. *Annu. Rev. Biophys. Biomol. Struct.* 21:267–92.

Luddens, H., and W. Wisden. 1991. Function and pharmacology of multiple $GABA_A$ receptor subunits. *Trends Pharmacol. Sci.* 12:49–51.

Nayeem, N., T. P. Green, I. L. Martin, and E. A. Barnard. 1994. Quaternary structure of the native $GABA_A$ receptor determined by electron microscopic image analysis. *J. Neurochem.* 62:815–818.

Neher, E. 1992. Correcting for liquid junction potentials in patch clamp experiments. *In* Methods in Enzymology. Ion Channels, Vol. 207. Academic Press, San Diego. 123–131.

Rajendra, S., J. W. Lynch, K. D. Pierce, C. R. French, P. H. Barry, and P. R. Schofield. 1994. Startle disease mutations reduce the agonist sensitivity of the human inhibitory glycine receptor. *J. Biol. Chem.* 269:18739–18742.

Robinson, R. A., and R. H. Stokes. 1959. Electrolyte Solutions. Butterworths, London.

Staley, K. J., B. L. Soldo, and W. R. Proctor. 1995. Ionic mechanisms of neuronal excitation by inhibitory $GABA_A$ receptors. *Science.* 269: 977–981.

Stühmer, W. 1992. Electrophysiological recording from *Xenopus* oocytes. *In* Methods in Enzymology. Ion Channels, Vol. 207. Academic Press, New York. 319–345.

Villarroel, A., S. Herlitze, M. Koenen, and B. Sakmann. 1991. Location of a threonine residue in the alpha subunit M2 transmembrane segment that determines the ion flow through the acetylcholine receptor channel. *Proc. R. Soc. Lond. B Biol.* 243:69–74.

Whiting, P. J., R. M. McKernan, and K. A. Wafford. 1995. Structure and pharmacology of vertebrate $GABA_A$ receptor subtypes. *Int. Rev. Neurobiol.* 38:95–138.

Xu, M., and M. N. Akabas. 1996. Identification of channel lining residues in the M2 membrane-spanning segment of the $GABA_A$ receptor α_1 subunit. *J. Gen. Physiol.* 107:195–205.

Zhang, H.-G., R. H. ffrench-Constant, and M. B. Jackson. 1994. A unique amino acid of the *Drosophila* GABA receptor influences drug sensitivity by two mechanisms. *J. Physiol. (Lond.).* 479:65–75.

Zhang, S. J., and M. J. Jackson. 1993. GABA activated chloride channels in secretory nerve endings. *Science.* 259:531–534.

Zhang, H.-G., H.-J. Lee, T. Rocheleau, R. H. ffrench-Constant, and M. B. Jackson. 1995. Subunit composition determines picrotoxin and bicuculline sensitivity of *Drosophila* γ-aminobutyric acid receptors. *Mol. Pharmacol.* 48:835–840.